Bulb extracts of *Boophone disticha* induce hepatotoxicity by perturbing growth, without significantly impacting cellular viability

Werner Cordier*, Vanessa Steenkamp

Department of Pharmacology, School of Medicine, Faculty of Health Sciences, University of Pretoria, Pretoria, South Africa

***Corresponding author details**

Corresponding author: Dr Werner Cordier

E-mail address: werner.cordier@up.ac.za

Fax number: +27 12 319 2411

Postal address: Department of Pharmacology, Faculty of Health Sciences, School of Medicine, University of Pretoria, P.O.Box X323, Arcadia, 0007, Pretoria, South Africa

Highlights

- The methanol extract of *Boophane disticha* bulbs is more cytotoxic than the hot water extract.
- Both extracts follow a similar mechanism of cytotoxicity.
- Mitochondrial depolarisation occurs, with no oxidative stress.
- Fatty acid accumulation is present, which may predispose cells to steatotic changes.
- Cell growth is diminished, however, little cell death occurs.

Abstract

Introduction: Traditional remedies remain a prominent form of therapy in developing countries, such as South Africa. *Boophone disticha*, or the poison bulb, is used for the treatments of wounds. There is generally a lack of scientific evidence to support its safety or use. As hepatotoxicity is a major contributor to morbidity and mortality, and a leading factor in drug attrition during development, more emphasis should be placed on pre-clinical evaluation thereof. The aim of the study was to investigate the *in vitro* hepatotoxicity of an ethnomedicinal and organic extract of the bulbs.

Materials and methods: Hot water (ethnomedicinal) and methanol (organic) extracts were prepared and assayed on HepG2 hepatocarcinoma cells to assess for effects on cell density (sulforhodamine B staining), mitochondrial membrane potential (JC-1 ratiometry), reactive oxygen species levels (H_2-DCF-DA cleavage/activation), reduced glutathione levels (monocholorobimane adduct formation), fatty acid accumulation (nile red staining), lipid peroxidation (thiobarbituric acid reactive substances formation), caspase-3/7 activation (Ac-DEVD-AMC activation), adenosine triphosphate levels (chemiluminescence), cell viability (Annexin V-FITC/propidium iodide) and cellular kinetics (propidium iodide).

Results: Although cell density was reduced by both extracts (hot water extract IC_{50} = 51.39 µg/mL; methanol extract IC_{50} = 35.11 µg/mL), cell viability was not reduced to the same degree (6 – 10% after 24 h; ~2% at 72 h) after exposure to the IC_{50}'s. Furthermore, cellular kinetics was not significantly affected. Although mitochondria appeared to depolarize slightly, reactive oxygen species levels were reduced to below baseline. Reduced glutathione levels also decreased. Fatty acid levels increased, however, lipids did not peroxidise. Adenosine triphosphate levels increased, while caspase-3/7 activity was reduced to below baseline.

Discussion and conclusion: Extracts of *B. disticha* did not induce a loss of cell viability, however, notable reduction in cell density was apparent. While the methanol extract was more cytotoxic than the hot water extract, the latter still carries a risk should

it be chronically used. Although cellular kinetics were not affected, it is proposed that extracts may shift cells into a quiescent phase of non-proliferation which the assay is not sensitive enough to detect. The antiproliferative effect is likely in response to altered redox status. However, mitochondrial depolarisation did not increase free radical levels, with no lipid peroxidation as consequence. Furthermore, a propensity for fatty acid accumulation was observed, which carries the risk of hepatosteatotic detriments. The antiproliferative effect may delay repair of hepatic injury, and thus reduce quality of life. Further emphasis should be placed on early investigation of herbal remedies for their effects on hepatocellular functioning.

Keywords: *Boophone disticha*; cell cycle; herb-induced liver injury; hepatotoxicity; toxicity.

Abbreviations

$\Delta\psi m$ – mitochondrial membrane potential; λ_{em} – emission wavelength; λ_{ex} – excitation wavelength; Ac – blank-adjusted average absorbance of the negative control; As – blank-adjusted absorbance of the sample; ATP – adenosine triphosphate; DMSO – dimethyl sulfoxide; EDTA - ethylenediaminetetraacetic acid; EMEM – Eagle's Modified Dublecco's Medium; FCS – foetal calf serum; FIc – normalised, blank-adjusted average fluorescence of the negative control; FIs – normalised, blank-adjusted fluorescence of the sample; GSH – reduced glutathione; H_2-DCFDA-DA – dihydrogendichlorofluorescein diacetate; LIc – normalised, blank-adjusted average fluorescence of the negative control; LIs – normalised, blank-adjusted fluorescence of the sample; PBS – phosphate-buffered saline; Rc – blank-adjusted average fluorescence of the negative control; Rs – blank-adjusted fluorescence of the sample; ROS: reactive oxygen species; SRB – sulforhodamine B

Conflict of interest

No conflict of interest is identified.

Author contributions

Dr W Cordier conducted all experimentation and drafted the manuscript. Prof V Steenkamp reviewed the manuscript and acted as primary supervisor.

1. Introduction

Herbal remedies are used as alternatives to conventional medicines for various reasons, including cultural significance, accessibility and cost-effectiveness (Louw *et al*., 2002; Wintola and Afolayan, 2010). A misguided belief is often present: herbal remedies are safer than allopathic counterparts due to their natural origin (Wintola and Afolayan, 2010). Even though medicinal plants are used frequently for medicinal reasons, their toxicological profiles are poorly described or typically non-existent. As such, the general populace may be exposed to potential toxins without their knowledge. Reports of herb-induced liver injury are increasing worldwide (Su *et al*., 2012; Wai *et al*., 2007), however, underestimations are assumed due to the inherent diagnostic limitations of identifying the contributing agents (Su *et al*., 2012; Wai *et al*., 2007). Furthermore, patients do not always disclose herbal usage, making it difficult to address frequency (Wai *et al*., 2007).

The liver, as primary metabolic organ of the body, is susceptible to toxicity by xenobiotics (Jaeschke *et al*., 2002). During metabolic conversion of xenobiotics, various reactive metabolites may be formed that put strain on biomolecular processes (Corsini and Bortolini, 2013). These may invoke subsequent cytotoxicity dependent on mitochondrial toxicity, oxidative stress and perturbations of signaling pathways (Corsini and Bortolini, 2013). In doing so, the liver may systemically present with lower functionality and thus reduce quality of life (Verma and Kaplowitz, 2009). Pre-clinical assessment of organotoxicity may thus offer important information that could be used to describe potential risk of use.

The poison bulb, *Boophone disticha* (L.f.) Herb. (Amaryllidaceae), is used for treatment of wounds, headaches, abdominal pains and eye conditions throughout Africa. It is a well-described hallucinogen used during divination ceremonies (De Smet, 1996; Gadaga *et al*., 2011), and its abuse frequency has been increasing in Zimbabwe (Gadaga *et al*., 2011). Little to no information of its effect on hepatocellular viability is available according to the authors' knowledge. Amaryllidaceae-type isoquinolone alkaloids (0.31% of the bulb) have been identified as poisonous phytochemicals (De Smet, 1996; van Wyk *et al*., 2002), which induce cytotoxicity (Adewusi *et al*., 2012a; Jitsuno *et al*., 2009; Li *et al*., 2007; Silva *et al*., 2008). These include, among others, bulbispermine (Jitsuno *et al*., 2009), 6-hydroxycrinamine (Adewusi *et al*., 2012a), lycorine (Li *et al*., 2007) and vittatine (Silva *et al*., 2008).

The aim of the study was to investigate the effect of crude extracts of *B. disticha* on hepatocellular viability of HepG2 hepatocarcinoma cells, with emphasis on mechanisms of cytotoxicity.

2. Methodology

2.1. Collection and extraction of plant material

Bulbs of *B. disticha* were gifted from the South African National Biodiversity Institute of Pretoria, South Africa. Bulbs were cleaned, split open and allowed to air-dry at ambient temperature, after which they were ground to a fine powder (YellowLine Grinder, Merck Co.). The plant material was stored in amber containers until used.

Hot water (ethnomedicinal preparation) and methanol (organic preparation) extracts were prepared through maceration of plant material in either boiling distilled water or room temperature methanol, respectively, at 10% (w/v). Hot water extracts were stirred for 15 min to simulate tea-brewing, and allowed to cool to room temperature. Methanol extracts were sonicated for 30 min, agitated for 2 h and left overnight at 4°C. Methanol was replenished, the process repeated thrice from agitation and supernatants

combined. Both extracts were centrifuged (1000 *g*, 5 min) and filtered (0.22 µm) to remove particles. Hot water and methanol extracts were dried through lyophilization and rotary-evaporation, respectively. Crystalised methanol extracts were reconstituted in distilled water and lyophilized. Aliquots (25 mg/mL in dimethyl sulfoxide [DMSO]) were stored at -80°C and diluted in serum-free Eagle's Modified Dulbecco's Medium (EMEM) prior to use.

2.2. Cellular maintenance

The HepG2 hepatocarcinoma cell line (ATCC #HB-8065) was maintained in EMEM fortified with 10% foetal calf serum (FCS) and 1% penicillin/streptomycin in 75 cm^2 flasks at 37°C and 5% CO_2. Confluent (80%) flasks were washed with phosphate-buffered saline (PBS), and cells detached using Trypsin/Versene. Cells were harvested through centrifugation (200 *g*, 5 min), and counted using trypan blue exclusion. Cells were diluted in 10% FCS-fortified EMEM.

2.3. Exposure of cells to crude extracts

Cells (100 µL) were seeded into 96-well plates (2 x 10^4 cells/well) and incubated overnight to allow for attachment. Cells were exposed (100 µL prepared in FCS-free EMEM) to 0.4% DMSO (negative, vehicle control), crude extracts (half-log dilutions of 100 µg/mL) or the respective positive control for 72 h. Blanks (200 µL) of 5% FCS-fortified EMEM alone accounted for background noise and sterility. After exposure, hepatotoxic parameters were determined as described in Sections 2.4. to 2.9., which were conducted on a single plate with modifications of the method of Tonder *et al*. (2001).

2.4. Cellular density

Cell density was determined using the sulforhodamine B (SRB) protein staining assay (Vichai and Kirtikara, 2006). Staurosporine (10 µM in-reaction) was used as positive control. Cells were fixed with 50 µL trichloroacetic acid (50%) overnight at 4°C, washed thrice with slow-running tap water and stained using 100 µL SRB solution (0.057% in

1% acetic acid) for 30 min. Stained cells were washed thrice with 100 µL acetic acid (1%), air-dried and the dye dissolved with 200 µL Tris-buffer (10 mM, pH 7.4). Absorbance was measured at 510 nm (reference 630 nm) (Synergy 2, Bio-Tek Instruments, Inc.) and adjusted by subtracting the blanks. Percentage cell density relative to the negative control was expressed using the following equation:

$$\text{Cell density (\% relative to negative control)} = \frac{\text{As}}{\text{Ac}} \times 100$$

where, As = the blank-adjusted absorbance of the sample, and Ac = the blank-adjusted average absorbance of the negative control.

2.5. Mitochondrial membrane potential

Mitochondrial membrane potential (∆ψm) was determined through the ratio of red fluorescent J-aggregates (healthy cells) to green fluorescent JC-1 monomers (unhealthy cells) (van Tonder, 2011). Rotenone (100 nM) was used as positive control. Plates were exposed to 10 µM JC-1 for 2 h and the fluorescent intensity measured at λ_{ex} = 492 nm and λ_{em} = 590 nm (gain 1000) and λ_{ex} = 485 nm and λ_{em} = 520 nm (gain 1000). Fluorescent intensity was adjusted by subtracting the blanks and the ratio of JC-1 monomers to J-aggregates determined. The fold-change in ∆ψm relative to the negative control was expressed using the following equation:

$$\Delta\Psi\text{m (fold} - \text{change relative to negative control)} = \frac{\text{Rs}}{\text{Rc}}$$

where, Rs = the ratio of blank-adjusted fluorescent intensity of the sample, and Rc = the ratio of blank-adjusted average fluorescent intensity of the negative control.

2.6. Intracellular reactive oxygen species levels

Intracellular reactive oxygen species (ROS) levels were determined using the enzymatic conversion of dihydrodichlorofluorescein diacetate (H_2-DCF-DA) to fluorescent dichlorofluoroscein (van Tonder, 2011). Potassium peroxidisulfate (150 µM in-reaction)

was used as positive control. Plates were exposed to 10 µM H_2-DCFH-DA for 2 h and the fluorescent intensity measured at λ_{ex} = 485 nm and λ_{em} = 520 nm (gain 750) (FLUOstar Optima, BMG Labtech). Cells were counterstained with SRB to account for reduced cell density. Fluorescent intensity was adjusted by subtracting the blanks, normalised to cell density and the fold-change in ROS levels expressed relative to the negative control using the following equation:

$$\text{Intracellular ROS levels (fold} - \text{change relative to negative control)} = \frac{\text{FIs}}{\text{FIc}}$$

where, FIs = the normalised, blank-adjusted fluorescent intensity of the sample, and FIc = the normalised, blank-adjusted average fluorescent intensity of the negative control.

2.7. Intracellular reduced glutathione levels

Intracellular reduced glutathione (GSH) levels were determined using the monochlorobimane-GSH affuct formation assay (Cordier *et al*., 2013). n-Ethylmaleimide (10 µM in-reaction) was used as positive control. Plates were exposed to 16 µM monochlorobimane for 2 h and the fluorescent intensity measured at λ_{ex} = 355 nm and λ_{em} = 460 nm (gain 1250). Fold-change in GSH levels was determined as described in Section 2.6.

2.8. Intracellular fatty acid levels

Intracellular fatty acid levels were determined using the cellular accumulation of nile red as a measure of steatosis (Kiela *et al*., 2005). Oleic acid (200 µM in-reaction) was used as positive control. Plates were exposed to 10 µM nile red for 2 h and the fluorescent intensity measured at λ_{ex} = 544 nm and λ_{em} = 590 nm (gain 1000). Fold change in intracellular fatty acid levels was determined as described in Section 2.6.

2.9. Caspase-3/7 activity

Caspase-3/7 activity was determined using the Ac-DEVD-AMC cleavage assay by activated caspase-3/7 (van Tonder, 2011). Staurosporine (10 µM in-reaction) was used

as positive control. Plates were centrifuged (200 *g*, 5 min), medium replaced with 25 µL cold lysis buffer and incubated for 15 min on ice. Thereafter, 100 µL caspase-3 substrate buffer containing Ac-DEVD-AMC was added, plates incubated for 4 h at 37˚C and overnight at 4˚C. The fluorescent intensity was measured at λ_{ex} = 355 nm and λ_{em} = 460 nm (gain 750). Fluorescent intensity was adjusted by subtracting the blanks, standardized according to the relative cell density and the percentage caspase-3 activity relative to the negative control expressed using the following equation:

$$\text{Caspase} - 3 \text{ activity (fold} - \text{change relative to negative control)} = \frac{\text{FIs}}{\text{FIc}}$$

where, FIs = the standardized, blank-adjusted fluorescent intensity of the sample, and FIc = the standardized, blank-adjusted average fluorescent intensity of the negative control.

2.10. Lipid peroxidation

Lipid peroxidation was determined using the thiobarbituric acid reactive substances (TBARS) assay (Stern *et al*., 2010). HepG2 cells were seeded and exposed as per Section 2.3. The oxidant, AAPH (500 µM in-reaction), was used as positive control. Medium (200 µL) was aspirated into 5 mL tubes, and cells combined with the supernatant after detachment with 100 µL Trypsin/Versene. The cellular mixture was mixed with 100 µL trichloroacetic acid (16.5%) and 100 µL thiobarbituric acid (2.5% in 0.1 M sodium hydroxide and 50 µM ethylenediaminetetraacetic acid [EDTA]), and incubated in a waterbath (95°C) for 20 min. After heating, 250 µL butanol was added and the mixture vortex-mixed. The organic layer (100 µL) transferred into a white 96-well plate after separation from the aqueous phase. The fluorescent intensity was measured at λ_{ex} = 544 nm and λ_{em} = 590 nm (gain 750). Fluorescent intensity was adjusted by subtracting the blanks, standardised to the relative cell density and the fold-change determined as described in Section 2.6.

2.11. Adenosine triphosphate levels

Adenosine triphosphate (ATP) levels were determined using the ApoSENSOR™ ATP cell viability chemiluminescence kit (Corporation, 2015). HepG2 cells were seeded and exposed as per Section 2.3. Saponin (1% in-reaction) was used as positive control. Medium was replaced with 100 µL nucleotide-releasing buffer and incubated for 5 min while shaken. After cell lysis, 10 µL ATP monitoring enzyme was added. Plates were immediately measured using a chemiluminescence protocol. Luminescent intensity was adjusted by subtracting the blanks, standardised to the relative cell density and the fold-change of the ATP levels relative to the negative control expressed using the following equation:

$$\text{ATP levels (fold} - \text{change relative to negative control)} = \frac{\text{LIs}}{\text{LIc}}$$

where, LIs = the normalized, blank-adjusted luminescent intensity of the sample, and LIc = the normalised, blank-adjusted average luminescent intensity of the negative control.

2.12. Cell viability

Cells were seeded into 24-well plates at 1 x 10^5 cells/well as described earlier and exposed to the half-maximal inhibitory concentration (IC_{50}) of the crude extracts for 24 and 72 h. Positive controls included 50 nM rotenone for 24 h (apoptosis) and sonication in cold 70% ethanol for 5 min (necrosis). After exposure, the supernatant and trypsinized cells were collected, pooled and washed with PBS containing 1% FCS (200 *g* for 5 min). The pellet was resuspended in Annexin V-FITC binding buffer and stained with Annexin V-FITC (1:200 v/v) for 15 min in the dark. Cells were counterstained with 15 µM propidium iodide. Measurements were done flow cytometrically using FL1 (525 nm, FITC) and FL3 (620 nm, propidium iodide) with quadrant analysis.

2.13. Cell cycle

Cells were synchronized using the thymidine double block method. Semi-confluent cells in 75 cm^2 culture flasks were exposed to 3 mM thymidine in 10% FCS-fortified EMEM for 16 h, after which flasks were washed with PBS and replenished with 10% FCS-fortified EMEM for 10 h. Medium was replaced with 3 mM thymidine in 10% FCS-fortified EMEM for another 16 h, and harvested. Synchronised cells were seeded and exposed in 24-well plates as described in Section 2.4. Positive controls included FCS-depletion for 24 h (G1-block), 10 µM methotrexate for 14 h (S-block) and 20 µM curcumin for 14 h (G2/M-block). The supernatant and trypsinized cells were collected, pooled and washed with PBS containing 1% FCS (200 *g* for 5 min), and fixed with cold 70% ethanol while vortex-mixing for 30 sec. Cells were left at 4°C overnight, and centrifuged at 200 *g* for 5 min. The pellet was resuspended in staining solution (40 µg/ml propidium iodide, 0.1% Triton X-100 and 100 µg/ml DNA-free RNAse) for 40 min at 37°C. Cells were analysed flow cytometrically (Beckman FC500, Beckman Coulter) using FL3 and the data expressed in percentages using deconvolution software (MultiCycle V3.0 for Windows) into a sub-G1, G0/G1, S and G2/M-phase.

2.14. Statistical analysis

Experiments were conducted with a minimum of three biological and two technical replicates. Results were expressed as the mean ± the standard error of the mean (SEM), and statistically analysed using GraphPad Prism 5.0. Non-linear regression (variable slope) was used to determine the IC_{50}. Significant difference relative to the negative control was determined using i) Kruskall-Wallis and a post-hoc Dunn's test (for 96-well plate assays), and ii) two-way analysis of variance (ANOVA) and a post-hoc Bonferroni test (24-well plate assays). Significance was defined as $p < 0.05$.

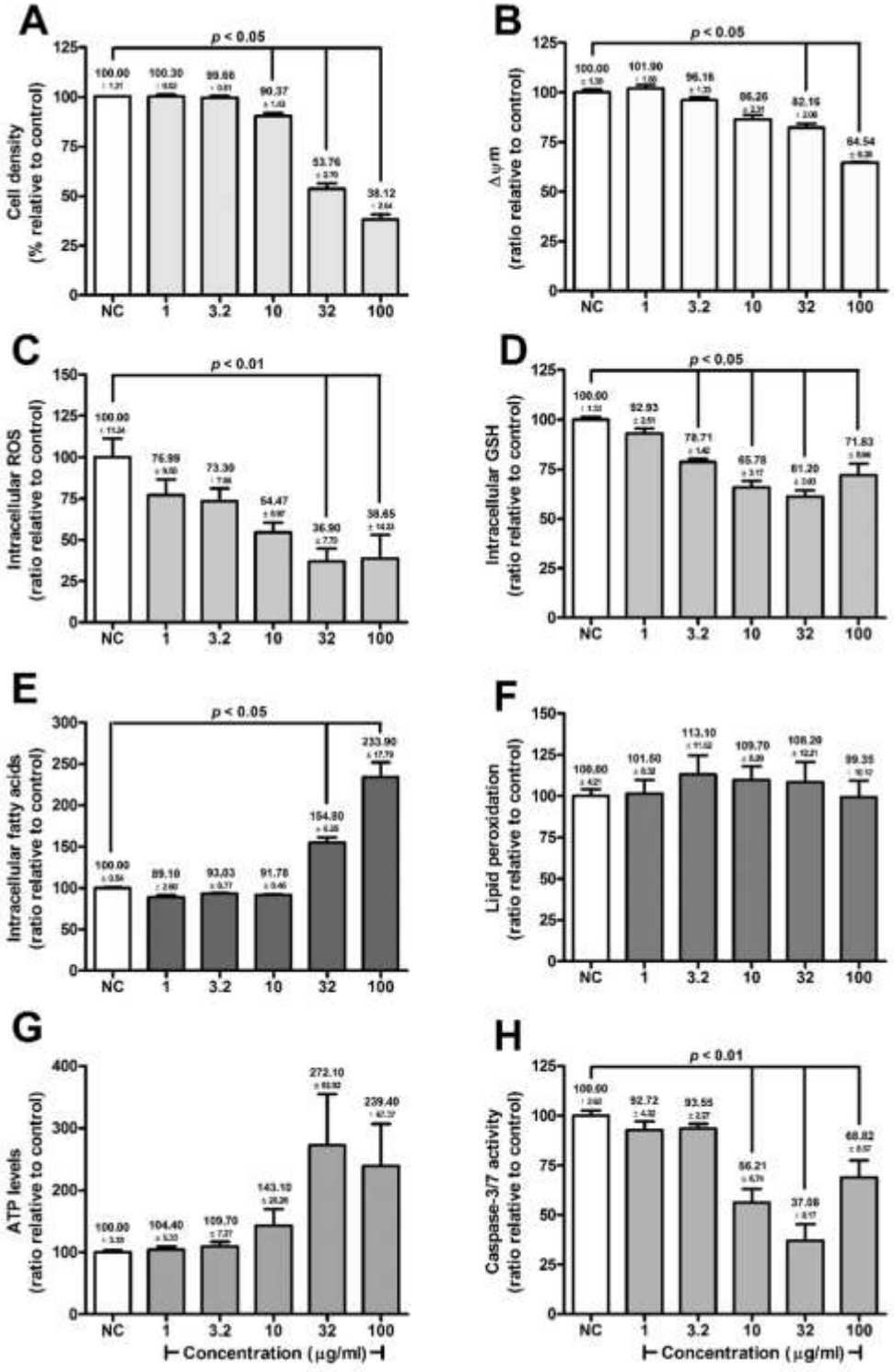

Figure 1: The effect of the hot water extract on HepG2 cells; A) cell density, B) $\Delta\Psi m$, C) ROS concentration, D) GSH concentration, E) fatty acid concentration, F) lipid peroxidation, G) ATP levels and H) caspase-3/7 activity.

3. Results

The hot water extract of *B. disticha* decreased cell density at ≥10 µg/mL, with an IC_{50} of 51.39 µg/mL (Figure 1A). The $\Delta\Psi m$ was decreased slightly ($p < 0.05$) at ≥32 µg/mL by up to 35.46% at 100 µg/mL (Figure 1B). Intracellular ROS concentrations were below baseline at all concentrations, with a reduction of 23.01% at 1 µg/mL which plateaued at ≥32 µg/mL by 63.10% (Figure 1C). Intracellular GSH concentrations decreased at ≥3.2 µg/mL by up to 38.80% ($p < 0.05$) (Figure 1D). Fatty acids accumulated dose-dependently at ≥10 µg/mL up to 233.90% at 100 µg/mL (Figure 1E). Lipid peroxidation was unperturbed relative to the negative control (Figure 1F), while ATP concentrations were non-significantly increased up to 272.10% at ≥32 µg/mL (Figure 1G). Caspase-3/7 activity was reduced at all concentrations in comparison to the negative control, however, this effect was not significant and less pronounced at 100 µg/mL (31.18%, Figure 1H).

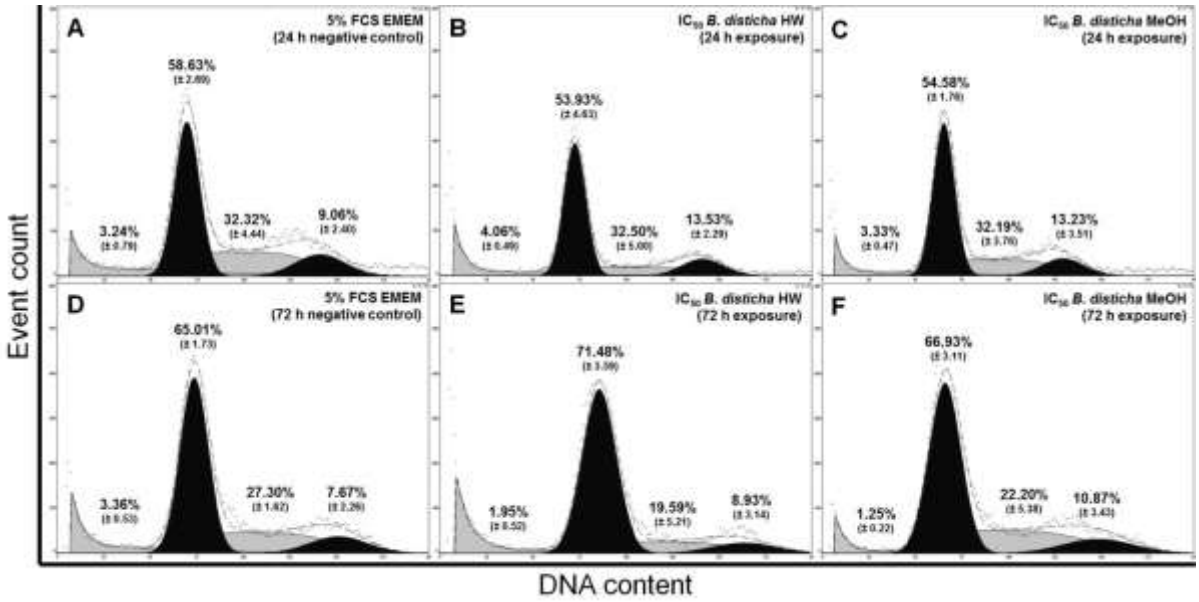

Figure 2: The effect of the IC_{50} on the cell cycle of HepG2 cells exposed for 24 h and 72 h; A) negative control (24 h), B) hot water extract (24 h), C) methanol extract (24 h), D) negative control (72 h), E) hot water extract (72 h), F) methanol extract (72 h). From the left hand side, each graph represents the distribution of cells in the sub-G1-, G0/G1-phase, S-phase and G2/M-phase as measured by propidium iodide-staining.

Although slight reductions in the percentage of cells in the sub-G1-, S- and G2/M-phase were observed after exposure to the hot water extract for 24 h, the G0/G1- and G2/M-phases increased by 6.47% and 1.24% after 72 h, respectively (Figure 2B, E), in comparison to the negative control. Relative to the negative control. an initial (24 h) decrease of 6.18% (p<0.05) in cell viability was observed due to apoptosis (8.43%), though this normalised after 72 h exposure to a 3.17% decrease (Figure 3B, E).

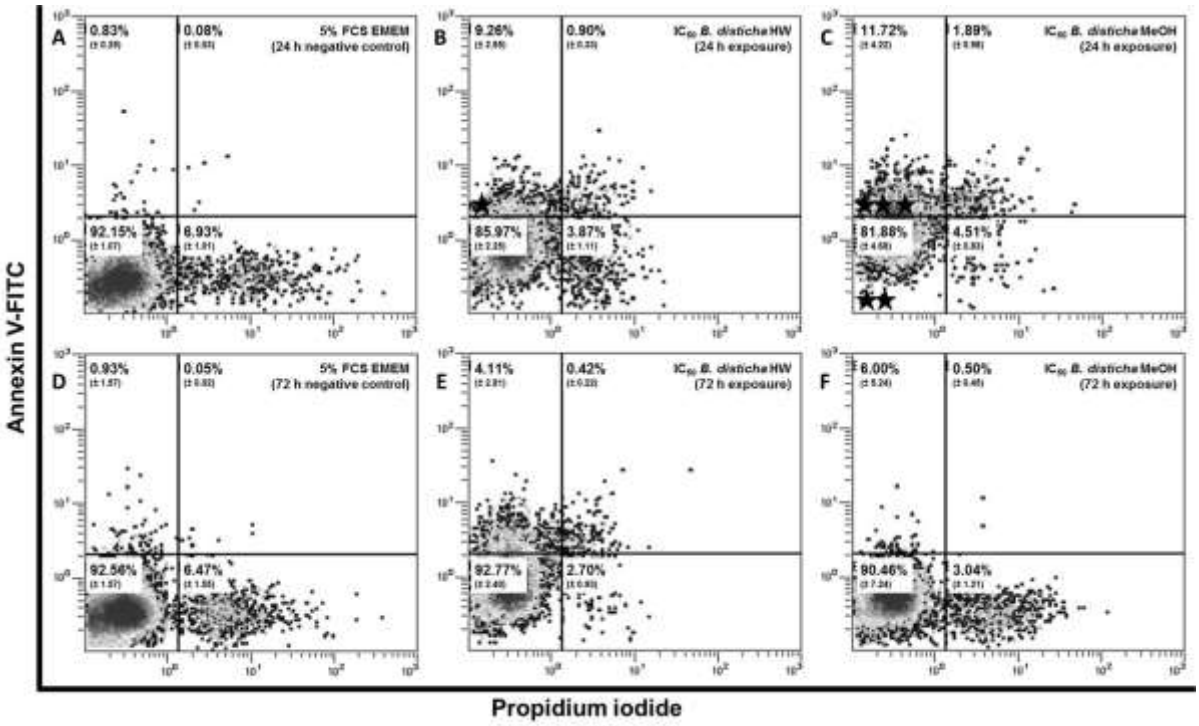

Figure 3: The effect of the IC_{50} on cellular viability in HepG2 cells exposed for 24 h and 72 h; A) negative control (24 h), B) hot water extract (24 h), C) methanol extract (24 h), D) negative control (72 h), E) hot water extract (72 h), F) methanol extract (72 h). Significant difference relative to the respective time points of the negative control: ★ $p < 0.05$, ★★ $p < 0.01$ and ★★★ $p < 0.001$. An increase in Annexin V-FITC-staining is indicative of cells undergoing apoptosis, while an increase in propidium iodide-staining suggests loss of membrane integrity as an indication of necrosis.

The methanol extract reduced cell density to a higher degree than the hot water extract, with an IC_{50} of 35.11 µg/mL. However, the maximum decrease in cell density at 100 µg/mL (66.43%) was similar to the hot water extract (61.88%) (Figure 4A). The $\Delta\Psi m$ decreased gradually by up to 43.39% (p<0.01) at 100 µg/mL (Figure 4B). Similar to the hot water extract, intracellular ROS concentrations were below baseline at all

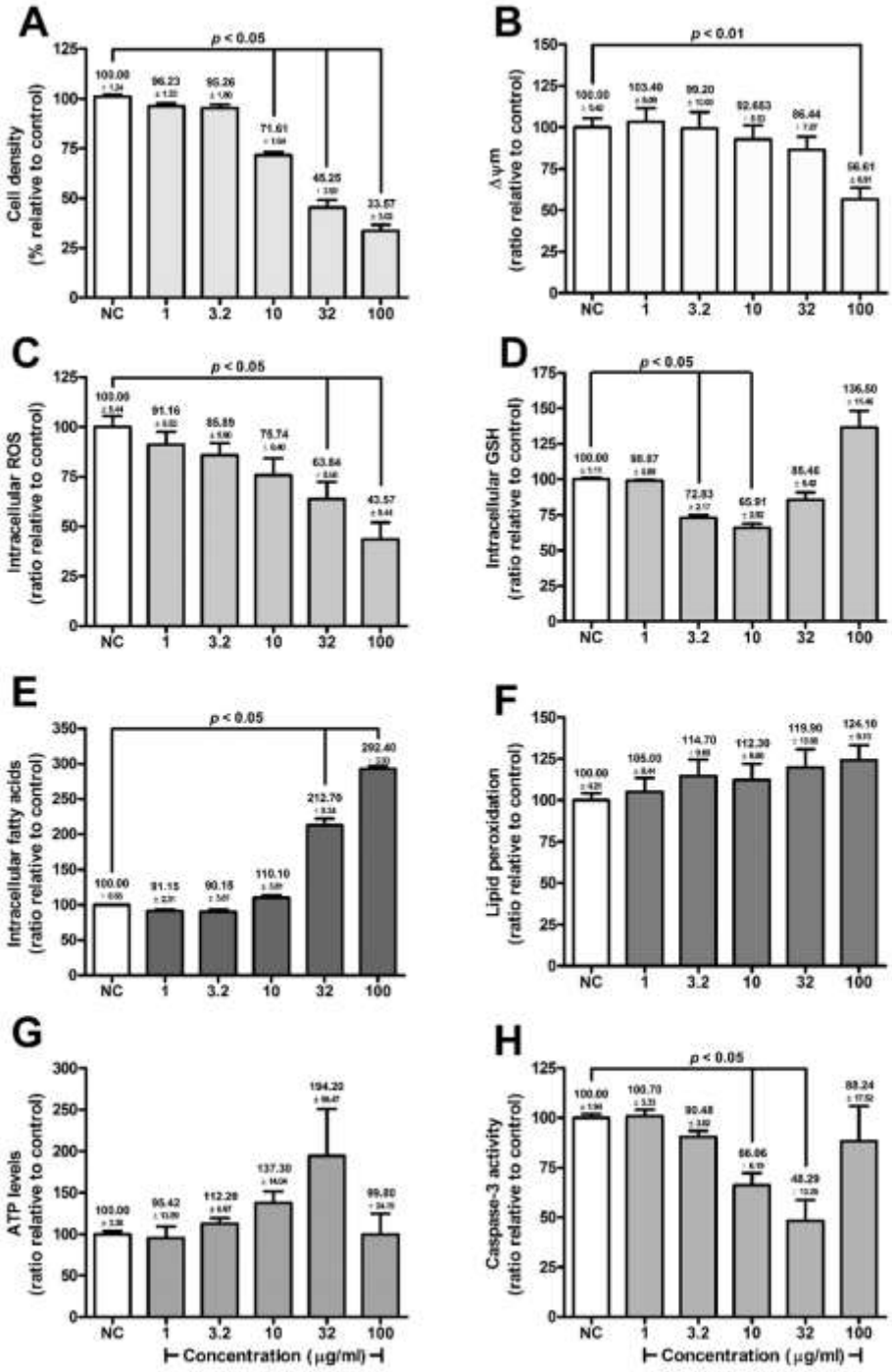

Figure 4: The effect of the crude methanol extract on HepG2 cells; A) cell density, B) ΔΨm, C) ROS concentration, D) GSH concentration, E) fatty acid concentration, F) lipid peroxidation, G) ATP levels and H) caspase-3/7 activity.

concentrations, by up to 56.43% at 100 µg/mL (Figure 4C). Intracellular GSH concentrations were reduced (p<0.001) at 3.2 µg/mL and 10 µg/mL by 27.17% and 34.09%, while at ≥32 µg/mL it dose-dependently increased by 136.50% at 100 µg/mL (Figure 4D). Fatty acids accumulated (p<0.05) by 292.40% at 100 µg/mL (Figure 4E), with non-significant dose-dependent increases in lipid peroxidation by up to 124.10% (Figure 4F). ATP levels were dose-dependently increased up to 137.30% at 10 µg/mL, it normalized to baseline at 100 µg/mL (Figure 4G). Caspase-3/7 activity was decreased (p<0.05) by 33.94%- and 51.71% at 10 µg/mL and 32 µg/mL, respectively, while only a 0.12-fold reduction was evident at 100 µg/mL (Figure 4H).

The methanol extract had a similar increase in the G0/G1- and G2/M-phase by 1.92% and 3.18%, respectively (Figure 2C, F), compared to the negative control. As with the hot water extract, the methanol extract initially (24 h) reduced cell viability by 10.27% (p<0.01) due to apoptosis (10.88%, p<0.001) (Figure 3C, F). After 72 h exposure, only a 2.10% reduction was observed, while early apoptotic cells increased by 5.07% (Figure 3C, F) compared to the negative control.

4. Discussion

B. disticha presented with moderate cytotoxicity; the methanol extract was more potent than the hot water extract. Botha *et al*. (2005) supports the cytotoxicity of ethanol extracts of the inner scales of the bulb, where decreased ATP levels were detected in human neutrophils. Hot water extracts of the inner and outer scales, as well as ethanol extracts of the outer scales, were inactive (Botha *et al*., 2005). As the latter study did not normalise ATP to cell density, and differentiated between the scales of the bulb, it may explain the discrepancy between the results. Adewusi *et al*. (2012b) described similar cytotoxicity in the SH-SY5Y neuroblastoma cell line after exposure to the methanol root extract (IC_{50} ~25.5 µg/mL) (Adewusi *et al*., 2012b). *In vivo*, liver weight increased in rats after acute hydroethanol extract treatment, while no histological alterations were observed. Authors suggested this to be due to adaptive *de novo* synthesis of liver

enzymes (Gadaga, 2012). Although reductions in cell density were evident, it appears that greater cytostatic effects are taking place than cell death. This was evident by the reduction of cell density, paralleled by low reductions in cell viability. Interestingly, cellular kinetics were largely unperturbed. Taking into account the lack of cell death and unperturbed cycling, it is suggested that a transition of proliferative cells to a quiescent G0-state took place. Propidium iodide does not differentiate between the diploid state of G0- and G1-phase cells (Darzynkiewicz *et al*., 2004), and thus measurement takes place as one phase. Cells are thus metabolically active, though not actively cycling (Cooper, 2000), which gives insight into the reduced cellular parameters. This assumption, however, needs to be ascertained using proliferative assays, such as a Ki-67-staining (Checker *et al*., 2015). Quiescence may be induced through a downregulation of cyclin D, or induction of p27 (Gemin *et al*., 2005), possibly as a consequence of mitogen-activated protein kinases (MAPK)-attenuation (Son *et al*., 2011). Reduced proliferation may impair hepatic regeneration and healing

Both extracts displayed a similar hepatotoxic effect following the same modality. Weak mitochondrial depolarisation occurred, suggestion a gradual or low-level opening of the membrane transition permeability pore (Begriche *et al*., 2011). The absence of ATP depletion supports this, as gradual opening would not lead to large-scale mitochondrial dysfunction. The increase in ATP at ≥10 µg/mL (which paralleled reduced cell density), suggests an adaptive promotion of bioenergetics for detoxification and efflux of phytotoxins. The reduction of ATP at 100 µg/mL methanol extract suggest a tipping point in cytotoxicity, where detrimental effects surpassed protective adaptation. Although depolarisation occurred, ROS concentrations did not increase, but decreased below baseline. Extracts have been shown to decrease superoxide production in neutrophils (Botha *et al*., 2005), which gives credence to the present study. As ROS functions as a signaling molecule, this suggests potential dysfunction of signalling cascades (Vivancos *et al*., 2010). Supporting the cytostatic effects, diminished ROS levels incur reduced transition to the S-phase of the cell cycle as oxidation is required (Vivancos *et al*., 2010). The parallel decrease of GSH levels suggests detoxification via phase II reactions (Zamek-Gliszczynski *et al*., 2006) rather than an antioxidant effect, as

no evidence of oxidation was observed. An increase of GSH at 100 µg/mL methanol extract exposure is likely an adaptive *de novo* synthesis response (Vivancos *et al*., 2010). Although mitochondrial dysfunction was not apparent, fatty acid accumulation systems were interrupted, as seen by the dose-dependent increase. This effect may be a function of β-oxidation enzyme inhibition (such as acyl-CoA synthases), cofactor depletion (Bartlett and Eaton, 2004; Pessayre *et al*., 2012), inhibited efflux systems or increased fatty acid synthesis/uptake (Pessayre *et al*., 2012). Although fatty acid levels increased, no significant lipid peroxidation was observed as ROS generation did not occur. While both extracts reduced caspase-3/7 activity, a small, initial increase in early apoptotic cells was observed, which could occur via caspase-independent means, such as non-caspase proteases (Schrader *et al*., 2010). As activity normalized at 100 µg/mL, this supports a tipping point in cytotoxicity, where different pathways are activated at high enough concentrations.

B. disticha belongs to the Amaryllidaceae family, which suggests isoquinoline-alkaloids as the bioactive, cytotoxic phytochemicals. While buphanadrine (Nair *et al*., 2012), buphanamine and buphanisine (Van Goietsenoven *et al*., 2010) are not regarded as highly cytotoxic, 6-hydroxycrinamine (Adewusi *et al*., 2012a), distichamine (Nair *et al*., 2012) and lycorine (Cao *et al*., 2013; Doskočil *et al*., 2015; Li *et al*., 2012, 2007; Van Goietsenoven *et al*., 2010) are likely contributors to the cytotoxicity observed. Lycorine acts as an antiproliferative (Cao *et al*., 2013; Li *et al*., 2012; Van Goietsenoven *et al*., 2010) and pro-apoptotic agent (Li *et al*., 2007). Distichamine has exerts antiproliferative effects in the low micromolar range (Nair *et al*., 2012). Alternatively, anthrones and saponins (identified via thin layer chromatography, results not shown) decrease cell growth as well. Derivatives of anthralin, an antiproliferative anthrone (Kratz *et al*., 2010; Müller *et al*., 1995) displays growth inhibitory effects without incurring cytotoxic effects (Kratz *et al*., 2010). Saponins reduce proliferation and induce apoptosis in the HepG2 cell line (Cristina *et al*., 2015; Li *et al*., 2014; Lu *et al*., 2015). It is likely a combinational effect of several chemical entities which are inducing the effects seen.

5. Conclusion

It is suggested that a mixture of phytochemicals promoted cytostatic effects, preventing HepG2 cells from proliferating in the absence of cell death. Such effects may reduce healing of injury that take place in the liver, with subsequent downstream implications on health. As *B. disticha* remains a popular ethnomedicinal preparation in Africa, caution should be used during use, specifically as the hot water extract had a similar mechanism by which it induced cytostatic responses. Furthermore, the pro-steatotic effects of extracts, such as in the present study, should be investigated further as it may promote inflammatory hepatitis and reduced quality of life. Larger emphasis should be placed on pre-clinical screening of herbal extracts against liver toxicity as little information is present.

6. Acknowledgements

The authors would like to acknowledge the contributions of Prof AD Cromarty (Department of Pharmacology), Dr JJ van Tonder (Triclinium Clinical Development) and Dr T Hurrell (Department of Physiology and Pharmacology, Karolinska Institutet) for their technical advice. Funding was obtained from the National Research Foundation associated with Dr Cordier's Thuthuka PhD Track grant (TTK1207112615).

7. References

Adewusi, E., Fouche, G., Steenkamp, V., 2012a. Cytotoxicity and acetylcholinesterase inhibitory activity of an isolated crinine alkaloid from *Boophone disticha* (Amaryllidaceae). J. Ethnopharmacol. 143, 572–528.

Adewusi, E., Fouche, G., Steenkamp, V., 2012b. Antioxidant, acetylcholinesterase inhibitory activity and cytotoxicity assessment of the crude extracts of *Boophone disticha*. African J. Pharmacol. Ther. 1, 78–83.

Bartlett, K., Eaton, S., 2004. Mitochondrial beta-oxidation. Eur. J. Biochem. 271, 462–469.

Begriche, K., Massart, J., Robin, M.-A., Borgne-Sanchez, A., Fromenty, B., 2011. Drug-

induced toxicity on mitochondria and lipid metabolism: mechanistic diversity and deleterious consequences for the liver. J. Hepatol. 54, 773–794.

Botha, E.W., Kahler, C.P., Plooy, W.J., Plooy, S.H., Mathibe, L., 2005. Effect of *Boophone disticha* on human neutrophils. J. Ethnopharmacol. 96, 385–388.

Cao, Z., Yu, D., Fu, S., Zhang, G., Pan, Y., Bao, M., Tu, J., Shang, B., Guo, P., Yang, P., Zhou, Q., 2013. Lycorine hydrochloride selectively inhibits human ovarian cancer cell proliferation and tumor neovascularization with very low toxicity. Toxicol.Lett. 218, 174–185.

Checker, R., Gambhir, L., Sharma, D., Kumar, M., Sandur, S.K., 2015. Plumbagin induces apoptosis in lymphoma cells via oxidative stress mediated glutathionylation and inhibition of mitogen-activated protein kinase phosphatases (MKP1/2). Cancer Lett. 357, 265–278.

Cooper, G., 2000. The Cell Cycle, in: The Cell: A Molecular Approach. Sinauer Associates.

Cordier, W., Gulumian, M., Cromarty, A., Steenkamp, V., 2013. Attenuation of oxidative stress in U937 cells by polyphenolic-rich bark fractions of *Burkea africana* and *Syzygium cordatum*. BMC Complement. Altern. Med. 13, 116–127.

Corporation, M.I., 2015. ApoSENSOR ATP Cell Viability.

Corsini, A., Bortolini, M., 2013. Drug-induced liver injury: The role of drug metabolism and transport. J. Clin. Pharmacol. 53, 463–474.

Cristina, T., Cogliati, B., Latorre, A.O., Akisue, G., Nagamine, M.K., Haraguchi, M., Hansen, D., Sanches, D.S., Lúcia, M., Dagli, Z., 2015. Pfaffosidic fraction from *Hebanthe paniculata* induces cell cycle arrest and caspase-3-induced apoptosis in HepG2 cells. Evidence-Based Complement. Altern. Med. 1–9.

Darzynkiewicz, Z., Crissman, H., Jacobberger, J.W., 2004. Cytometry of the cell cycle: cycling through history. Cytom. Part A 58A, 21–32.

De Smet, P., 1996. Some ethnopharmacological notes on African hallucinogens. J. Ethnopharmacol. 50, 141–146.

Doskočil, I., Hošťálková, A., Šafratová, M., Benešová, N., Havlík, J., Havelek, R., Kuneš, J., Královec, K., Chlebek, J., Cahlíková, L., 2015. Cytotoxic activities of Amaryllidaceae alkaloids against gastrointestinal cancer cells. Phytochem. Lett. 13, 394–398.

Gadaga, L., Tagwireyi, D., Dzangare, J., Nhachi, C., 2011. Acute oral toxicity and neurobehavioural toxicological effects of hydroethanolic extract of *Boophone disticha* in rats. Hum. Exp. Toxicol. 30, 972–980.

Gadaga, L.L., 2012. Investigation of the toxicological and pharmacological activity of a hydroethanolic extract of *Boophone disticha* bulb. University of Zimbabwe Thesis.

Gemin, a, Sweet, S., Preston, T.J., Singh, G., 2005. Regulation of the cell cycle in response to inhibition of mitochondrial generated energy. Biochem Biophys Res Commun 332, 1122–1132.

Jaeschke, H., Gores, G.J., Cederbaum, A.I., Hinson, J. a, Pessayre, D., Lemasters,

J.J., 2002. Mechanisms of hepatotoxicity. Toxicol. Sci. 65, 166–76.

Jitsuno, M., Yokosuka, A., Sakagami, H., Mimaki, Y., 2009. Chemical constituents of the bulbs of *Habranthus brachyandrus* and their cytotoxic activities. Chem. Pharm. Bull. (Tokyo). 57, 1153–7.

Kiela, P.R., Midura, A.J., Kuscuoglu, N., Jolad, S.D., Sólyom, A.M., Besselsen, D.G., Timmermann, B.N., Ghishan, F.K., 2005. Effects of *Boswellia serrata* in mouse models of chemically induced colitis. Am. J. Physiol. Gastrointest. Liver Physiol. 288, G798-808.

Kratz, U., Prinz, H., Müller, K., 2010. Synthesis and biological evaluation of novel 10-benzyl-substituted 4,5-dichloro-10H-anthracen-9-ones as inhibitors of keratinocyte hyperproliferation. Eur. J. Med. Chem. 45, 5278–85.

Li, L., Dai, H.-J., Ye, M., Wang, S.-L., Xiao, X.-J., Zheng, J., Chen, H.-Y., Luo, Y.-H., Liu, J., 2012. Lycorine induces cell-cycle arrest in the G0/G1 phase in K562 cells via HDAC inhibition. Cancer Cell Int. 12, 49.

Li, Y., Liu, J., Tang, L.J., Shi, Y.W., Ren, W., Hu, W.X., 2007. Apoptosis induced by lycorine in KM3 cells is associated with the G0/G1 cell cycle arrest. Oncol.Rep. 17, 377–384.

Li, Y., Man, S., Li, J., Chai, H., Fan, W., Liu, Z., Gao, W., 2014. The antitumor effect of formosanin C on HepG2 cell as revealed by 1H-NMR based metabolic profiling. Chem. Biol. Interact. 220, 193–199.

Louw, C., Regnier, T., Korsten, L., 2002. Medicinal bulbous plants of South Africa and their traditional relevance in the control of infectious diseases. J. Ethnopharmacol. 82, 147–154.

Lu, J.-J., Lu, D.-Z., Chen, Y.-F., Dong, Y.-T., Zhang, J.-R., Li, T., Tang, Z.-H., Yang, Z., 2015. Proteomic analysis of hepatocellular carcinoma HepG2 cells treated with platycodin D. Chin. J. Nat. Med. 13, 673–679.

Müller, K., Leuekl, P., Mayer, K., Wiegrebe, W., 1995. Modification of DNA bases by anthralin and related compounds. Biochem. Pharmacol. 49, 1607–1613.

Nair, J.J., Rárová, L., Strnad, M., Bastida, J., van Staden, J., 2012. Apoptosis-inducing effects of distichamine and narciprimine, rare alkaloids of the plant family Amaryllidaceae. Bioorg. Med. Chem. Lett. 22, 6195–6199.

Pessayre, D., Fromenty, B., Berson, A., Robin, M.-A., Lettéron, P., Moreau, R., Mansouri, A., 2012. Central role of mitochondria in drug-induced liver injury. Drug Metab. Rev. 44, 34–87.

Schrader, K., Huai, J., Jöckel, L., Oberle, C., Borner, C., 2010. Non-caspase proteases: Triggers or amplifiers of apoptosis? Cell. Mol. Life Sci. 67, 1607–1618.

Silva, A.F, de Andrade, J.P., Machado, K.R., Rocha, A.B., Apel, M.A., Sobral, M.E., Henriques, A.T., Zuanazzi, J.A., 2008. Screening for cytotoxic activity of extracts and isolated alkaloids from bulbs of *Hippeastrum vittatum*. Phytomedicine 15, 882–885.

Son, Y., Cheong, Y., Kim, N., Chung, H., Kang, D.G., Pae, H., 2011. Mitogen-activated

protein kinases and reactive oxygen species: How can ROS activate MAPK pathways. J. Signal Transduct. 2011.

Stern, S., Potter, T., Neun, B., 2010. NCL method GTA-4: Hep G2 hepatocyte lipid peroxidation assay. Nanotechnol. Charact. Lab.

Su, Y.-W., Chen, X., Jiang, Z.-Z., Wang, T., Wang, C., Zhang, Y., Wen, J., Xue, M., Zhu, D., Zhang, Y., Su, Y.-J., Xing, T.-Y., Zhang, C.-Y., Zhang, L.-Y., 2012. A panel of serum microRNAs as specific biomarkers for diagnosis of compound- and herb-induced liver injury in rats. PLoS One 7, e37395.

Van Goietsenoven, G., Andolfi, A., Lallemand, B., Cimmino, A., Lamoral-Theys, D., Gras, T., Abou-Donia, A., Dubois, J., Lefranc, F., Mathieu, V., Kornienko, A., Kiss, R., Evidente, A., 2010. Amaryllidaceae alkaloids belonging to different structural subgroups display activity against apoptosis-resistant cancer cells. J. Nat. Prod. 73,

van Tonder, J., 2011. Development of an in vitro mechanistic toxicity screening model using cultured hepatocytes. University of Pretoria thesis.

van Wyk, B.-E., van Heerden, F., van Oudtshoorn, B., 2002. Poisonous plants of South Africa, First Edit. ed. Briza Publications, South Africa.

Verma, S., Kaplowitz, N., 2009. Diagnosis , management and prevention of drug-induced liver injury. Gut 58, 1555–1564.

Vichai, V., Kirtikara, K., 2006. Sulforhodamine B colorimetric assay for cytotoxicity screening. Nat. Protoc. 1, 1112–1116.

Vivancos, P., Wolff, T., Markovic, J., Pallardó, F., Foyer, C., 2010. A nuclear glutathione cycle within the cell cycle. Biochem J 431, 169–178.

Wai, C.-T., Tan, B.-H., Chan, C.-L., Sutedja, D.S., Lee, Y.-M., Khor, C., Lim, S.-G., 2007. Drug-induced liver injury at an Asian center: a prospective study. Liver Int. 27, 465–74.

Wintola, O., Afolayan, A., 2010. Ethnobotanical survey of plants used for the treatment of constipation within Nkonkobe Municipality of South Africa. African J. Biotechnol. 9, 7767–7770.

Zamek-Gliszczynski, M.J., Hoffmaster, K. a., Nezasa, K.I., Tallman, M.N., Brouwer, K.L.R., 2006. Integration of hepatic drug transporters and phase II metabolizing enzymes: Mechanisms of hepatic excretion of sulfate, glucuronide, and glutathione metabolites. Eur. J. Pharm. Sci. 27, 447–486.